Future Development of Contrail Cover, Optical Depth, and Radiative Forcing: Impacts of Increasing Air Traffic and Climate Change

S. MARQUART, M. PONATER, F. MAGER, AND R. SAUSEN

Deutsches Zentrum für Luft- und Raumfahrt, Institut für Physik der Atmosphäre, Oberpfaffenhofen, Germany

(Manuscript received 23 October 2002, in final form 25 February 2003)

ABSTRACT

The future development of contrails is investigated considering changes in air traffic and aircraft technology as well as climate change by means of a contrail parameterization developed for the ECHAM general circulation model. Time slice simulations show an increase in global annual mean contrail cover from 0.06% in 1992, to 0.14% in 2015, and to 0.22% in 2050. In the northern extratropics, the enhancement of contrail cover is mainly determined by the growth of aviation. In the Tropics, contrail cover is, additionally, highly affected by climate change. In order to quantify the effect of systematic errors in the model climate on contrail cover, offline diagnostic studies are also performed. These studies suggest an underestimation of global contrail cover in the ECHAM simulations by a factor of about 0.8–0.9. The effect of the bias in the model climate is strongest in tropical latitudes. The temporal development of the simulated contrail radiative forcing is most closely related to total contrail cover, although the mean optical depth is found to increase in a warmer climate. Our best estimate is an increase of global annual mean radiative forcing from 3.5 mW m^{-2} in 1992, to 9.4 mW m^{-2} in 2015, and to 14.8 mW m^{-2} in 2050. Uncertainties in contrail radiative forcing mainly arise from uncertainties in microphysical and optical properties such as particle shape, particle size, and optical depth.

1. Introduction

Anthropogenic changes in cirrus cloudiness such as line-shaped contrails, contrail–cirrus, or indirectly induced cirrus from accumulating particle emissions may have a significant influence on the earth's climate system (Schumann and Ström 2001). The Intergovernmental Panel on Climate Change (IPCC) special report ''Aviation and the Global Atmosphere'' (Penner et al. 1999) provided an estimate for the radiative forcing of linear contrails in the range of 0.02 W m^{-2} for 1992, amounting to 40% of the total radiative forcing from aviation impacts. Assuming IPCC aviation scenario Fa1, radiative forcing due to contrails will have increased to 0.1 W m^{-2} by 2050, which then would amount to about 50% of the total aircraft radiative forcing (Penner et al. 1999). A large uncertainty range of roughly a factor of 4 was associated with the radiative forcing of line-shaped contrails, based on sensitivity considerations discussed in Minnis et al. (1999).

Since the Penner et al. (1999) report, a variety of studies on contrails have been published both from the observational and from the model-based point of view. An algorithm developed by Mannstein et al. (1999), which allows for an operational detection of line-shaped contrails from satellite data, was used to quantify contrail cover over different regions of the world (Minnis et al. 2000; Meyer et al. 2002a,b). Beyond the radiative transfer model calculations of Minnis et al. (1999), on which the Penner et al. (1999) radiative forcing estimates mainly rely, alternative model approaches were used to compute the radiative impact of contrails. In general, the more recent results (Myhre and Stordal 2001; Marquart and Mayer 2002; Meyer et al. 2002b) tend to be somewhat lower than the best estimate given by the IPCC report. Nevertheless, line-shaped contrails still have to be considered as an important factor of aircraft-induced climate change.

The expected increase in air traffic will certainly contribute to an increase in contrail cover. More efficient engines will lead to a colder exhaust gas and will, therefore, also facilitate contrail formation (Schumann 2000). These effects have already been studied by means of a diagnostic method based on the thermodynamic theory of contrail formation (Sausen et al. 1998; Gierens et al. 1999). The global mean contrail cover was estimated to increase from 0.09% in 1992, to about 0.2% in 2015, and 0.5% in 2050, assuming a nonchanging atmospheric environment. However, a warmer climate as expected during the twenty-first century (Houghton et al. 2001) would reduce the coverage of contrails, which form preferably in a sufficiently cold environment (Sausen 2000).

Corresponding author address: Dr. Susanne Marquart, Deutsches Zentrum für Luft- und Raumfahrt, Institut für Physik der Atmosphäre, Oberpfaffenhofen, D-82234 Wessling, Germany.
E-mail: Susanne.Marquart@dlr.de

In the present paper, we investigate the future development of contrails in a changing background climate by means of a contrail parameterization developed by Ponater et al. (2002) for the general circulation model (GCM) ECHAM4. We consider changes in air traffic and propulsion efficiency, as well as increasing greenhouse gas concentrations in the atmosphere for three time slices: 1992, 2015, and 2050. In contrast to the diagnostic approach of Sausen et al. (1998) the parameterization allows us to estimate online, within a self consistent framework, both coverage and optical properties of the contrails as well as the resulting radiative forcing.

However, the straightforward interpretation of the GCM results is restricted by model systematic errors in temperature and humidity distributions, which directly affects the thermodynamic contrail formation frequency. In order to quantify the effect of the bias in model climate on the computed contrail cover, the above-mentioned diagnostic Sausen et al. (1998) method is used for several sensitivity considerations.

The two approaches to determine contrail cover, that is, the GCM parameterization as well as the offline diagnostics, are described in section 2. In sections 3–5, results for future changes in contrail cover, optical depth, and radiative forcing are presented and discussed, with special emphasis given to the impact of systematic errors in the model climate. Finally, conclusions are presented in section 6.

2. Methods

The characteristic features of both the GCM parameterization (hereafter denoted as the ''online'' method) and the diagnostic approach (hereafter denoted as ''offline'' method), as well as the strategy in combining both methods favorably, are described in this section.

The GCM contrail parameterization was developed for the ECHAM4.L39 (DLR) model (Roeckner et al. 1996; Land et al. 1999, 2002), which we use in a horizontal spectral T30 resolution with a time step of 30 min. The model has 39 layers between the surface and the top layer centered at 10 hPa, resulting in a vertical resolution of about 700 m (or approximately 20 hPa) in the tropopause region where air traffic mainly occurs. The model was extended by a contrail parameterization scheme that is based on the thermodynamic theory of contrail formation (Ponater et al. 2002). Contrails may form at any time step depending on ambient temperature, humidity, and natural cloudiness, also considering actual air traffic movements. The simulated contrails are characterized by a fractional grid box coverage, an individual ice water path and effective particle size, and optical properties. For details, see Ponater et al. (2002).

The radiative forcing of contrails is determined as the difference of radiative fluxes with and without contrails. As a measure of climate impact we use the stratosphere-adjusted radiative forcing at the tropopause, which is calculated online in ECHAM4 (Stuber et al. 2001b). In contrast to Ponater et al. (2002), we do not rely on the standard ECHAM4 longwave radiation scheme for our radiative forcing calculations: Marquart and Mayer (2002) found that the longwave radiative forcing of optically thin ice clouds (such as contrails) is severely underestimated in the standard ECHAM4 radiation scheme. Therefore, we make use of an upgraded version of the longwave scheme (Marquart and Mayer 2002). Note that, for this reason, the values for radiative forcing given in the present paper are systematically higher than those presented by Ponater et al. (2002).

We perform so-called time slice simulations with fixed annual cycles of boundary conditions (sea surface temperature, solar radiation, and fixed concentrations of greenhouse gases) for each year considered. For the future time slice simulations (2015, 2050), changes in the background climate (with respect to 1992 conditions) are based on increasing greenhouse gas concentrations according to the scenario IS92a of the IPCC report (Houghton et al. 1992), as well as on corresponding sea surface temperature changes taken from a transient climate simulation with the coupled atmosphere–ocean model ECHAM4/OPYC (Roeckner et al. 1999). In this simulation, the global mean surface temperature rises by 2.6 K from 1992 to 2050. As we do not account for the potential damping influence of increasing tropospheric aerosol abundance on global warming, our climate change scenario is likely to represent an upper limit of tropospheric temperature increase.

Our offline diagnostic approach closely follows the lines described by Sausen et al. (1998). Contrail cover is calculated at fixed pressure levels (with 50-hPa resolution in the main flight altitudes) in a similar manner to the GCM's contrail parameterization. Daily values of temperature and relative humidity (with respect to ice) at 1200 UTC are employed. Besides 10 years of European Centre for Medium-Range Weather Forecasts (ECMWF) reanalysis data (ERA 1983–92; Gibson et al. 1997), which were also used by Sausen et al. (1998) and Gierens et al. (1999), we also apply climate model data to diagnose contrail cover: temperature and relative humidity values are extracted for three 10-yr periods (1985–94, 2010–19, and 2045–54) from the transient climate simulation with ECHAM4/OPYC mentioned above.

For both types of calculations, we use 3D inventories of fuel consumption as a measure of air traffic for the time slices 1992, 2015 [Deutsches Zentrum für Luft- und Raumfahrt (DLR) inventories; Schmitt and Brunner 1997], and 2050 [National Aeronantics and Space Administration (NASA) inventories, scenario FESGa; Baughcum et al. 1998; Penner et al. 1999]. In all inventories, subsonic aviation is assumed. The annual cycle of air traffic is included. The daily cycle is neglected in most calculations as it turned out to be only of minor importance on a global and annual mean scale (see section 5b). Concerning propulsion efficiencies we rely on

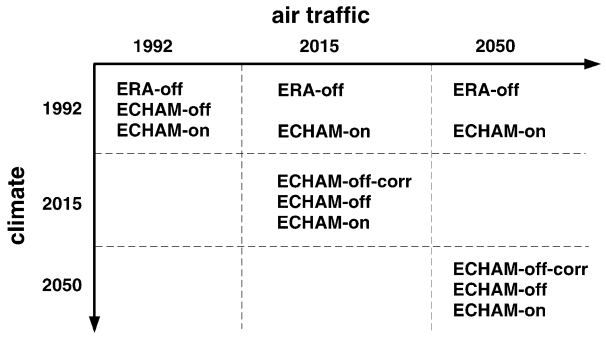

FIG. 1. Performed calculations, characterized by the respective assumptions about air traffic and climate. The studies allow us 1) to separate the effects of changes in air traffic and climate and 2) to quantify how systematic errors in the model climate affect contrail cover. The suffixes ''-on'' and ''-off'' denote online contrail simulations and offline calculations; ''ECHAM'' and ''ERA'' denote the underlying meteorological data.

considerations provided by Gierens et al. (1999), who anticipated a respective increase from 0.3 in 1992, to 0.4 in 2015, and to 0.5 in 2050.

In both cases, that is, the online GCM simulations and the offline diagnostic calculations, the mean contrail cover of the western Europe–east Atlantic region was calibrated to satellite observations of Bakan et al. (1994), in analogy to previous studies (Sausen et al. 1998; Gierens et al. 1999; Ponater et al. 2002). However, while all these studies were calibrated to the daytime mean coverage of 0.5% reported by Bakan et al. (1994) for the respective area, we rather use the more appropriate 24-h mean of 0.375%. Values for contrail cover presented in this paper are therefore expected to be about 25% lower than those provided by the above-mentioned studies.

The main objectives of the present paper are 1) to estimate future contrail cover, optical depth, and the resulting radiative forcing in a changing background climate; 2) to separate the effects resulting from future changes in air traffic and aircraft technology from those resulting from climate change; and 3) to quantify the sensitivity of contrail cover arising from the bias in the model climate. For these purposes, a variety of online simulations and offline calculations were performed for the three time slices and different combinations of air traffic, propulsion efficiency, and atmospheric environment. The most important simulations are shown schematically in Fig. 1 and will be explained in detail in the following sections.

Although the formal way of computing contrail coverage by means of the offline diagnostics is quite similar to the GCM's parameterization, the offline method contains some fundamental caveats. Information about ice water is only available within the framework of the GCM, allowing us to consider criteria like contrail persistence or visibility, in addition to the solely thermodynamical possibility of contrail formation. Following the approach of Ponater et al. (2002), in the current GCM simulations contrails are only retained in a grid box if they contain sufficient ice water to persist during a whole model time step. Furthermore, only those contrails are taken into account for calibration whose optical depth exceeds a ''visibility'' threshold value of 0.02. (Note, however, that ''nonvisible'' contrails still contribute—by 6%–7% in the global mean—to radiative forcing.) In the offline studies, however, such additional aspects cannot be considered; therefore, this approach has to be regarded as conceptually inferior to the GCM parameterization.

Nevertheless, the effect of the bias in model climate in the simulated contrail cover can be quantified most efficiently in offline studies, where meteorological data can easily be provided from external data sources. Therefore, while the GCM simulations allow for a comprehensive simulation of the coverage, optical properties, and radiative forcing of contrails, the offline method is a suitable additional tool to reduce uncertainties regarding the GCM computed contrail cover.

3. Contrail cover

a. Recent conditions and future projections

Contrail cover is determined in the GCM as a fractional coverage within each model grid box. Unless mentioned otherwise, we refer to the so-called ''visible'' contrail cover (Ponater et al. 2002), which comprises only contrails that exceed a minimal optical depth of 0.02 and are not obscured by natural clouds. These restrictions are consistent as the modeled contrail coverage is calibrated and compared to observed contrails, which are not detected below a certain threshold optical depth or directly beneath or underneath natural cirrus clouds.

Summing up vertically by using the principle of maximum-random overlap (e.g., Geleyn and Hollingsworth 1978), the total contrail cover is gained as a 2D distribution. As an example, Fig. 2 shows the annually averaged total contrail cover simulated for the time slice 1992. In this figure, regions are indicated for which observational data exist that can be and have already been compared with the model results (Ponater et al. 2002; Meyer et al. 2002a). The boundaries and the denotations of the regions are provided in the legend of Fig. 2. These regions will be the focus of our interest in the following sections. Marked in black is the region analyzed by Bakan et al. (1994), which is used for model calibration.

The top panels of Fig. 3 show how total contrail cover is expected to change in the future relative to the 1992 conditions. Both changes in air traffic (flight density as well as propulsion efficiency) and climate are considered. The calculated contrail cover is found to increase nearly all over the world. Global mean contrail cover more than doubles from 1992 to 2015 and increases further until 2050 by a factor of about 1.6.

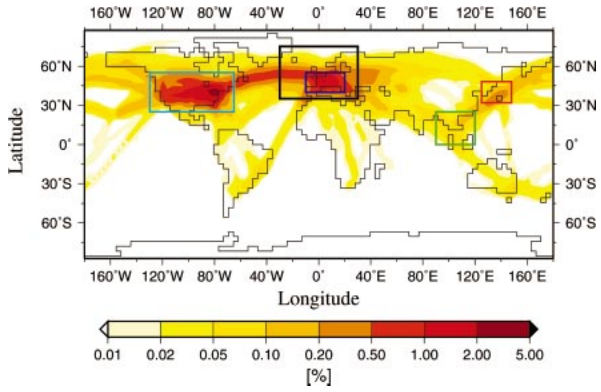

FIG. 2. Annually averaged total contrail cover (%) for the 1992 time slice simulated by ECHAM4. Regions for which satellite-based contrail observations exist are marked: black, western Europe–east Atlantic (35°–75°N, 30°W–30°E; Bakan et al. 1994); dark blue, western Europe (40°–55°N, 10°W–20°E; Meyer et al. 2002b); light blue, United States (25°–55°N, 130°–65°W; Minnis et al. 2000); red, Japan region (30°–48°N, 126°–148°E; Meyer et al. 2002a); green, Thailand region (0°–25°N, 90°–122°E; Meyer et al. 2002a).

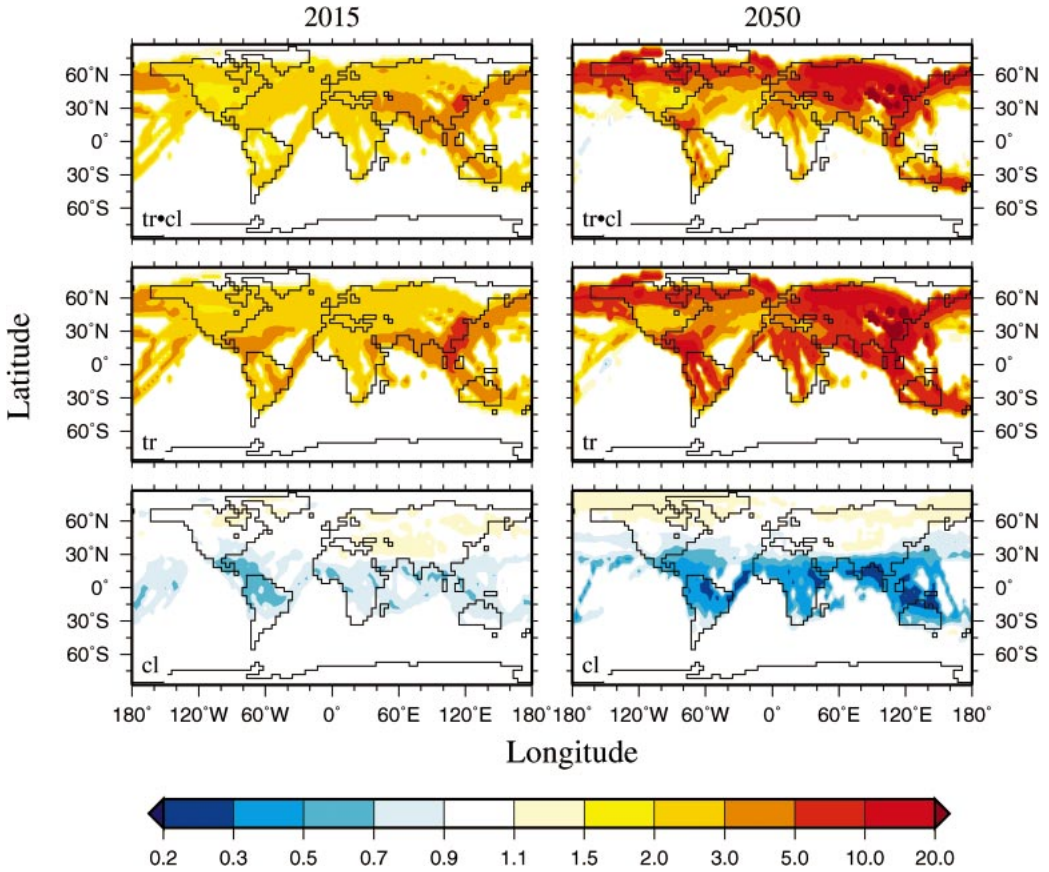

FIG. 3. Ratios of the annual mean contrail cover for different scenarios separating the effects of changes in air traffic (tr) and climate (cl). (top), (middle) Changes in contrail cover relative to the 1992 reference scenario, where (top) shows the overall effect: combined changes in air traffic and climate between (left) 2015 and 1992 and (right) 2050 and 1992; and (middle) shows the traffic effect: changes in air traffic only between (left) 2015 and 1992 and (right) 2050 and 1992. (bottom) Ratio of (top) and (middle) panels (climate effect). Please note that the overall effect (tr·cl), therefore, is the product of the climate effect (cl) and the traffic effect (tr).

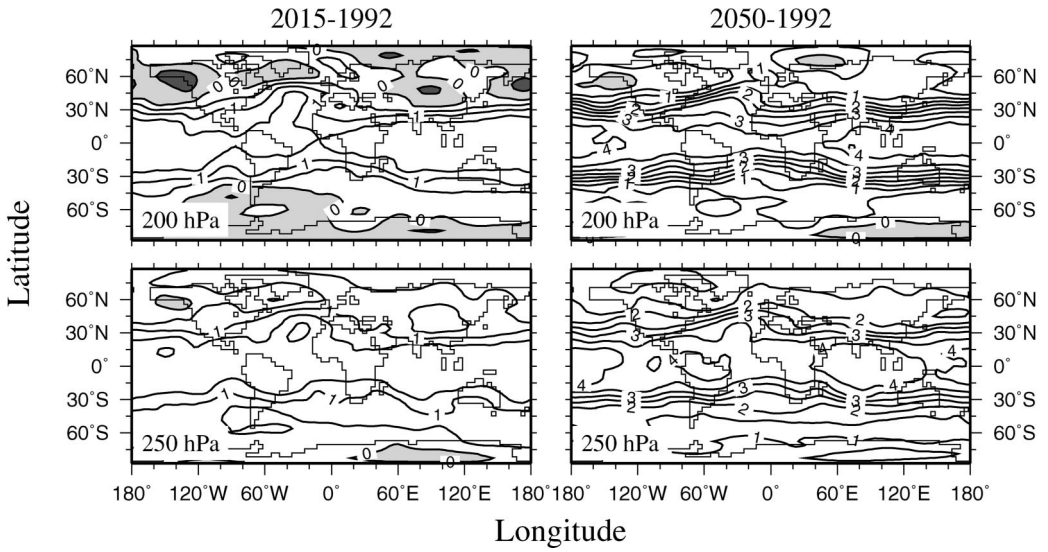

FIG. 4. Annual mean temperature difference (K) in the GCM simulations between (left) 2015 and 1992 and (right) 2050 and 1992 at (top) 200 and (bottom) 250 hPa. Isoline spacing is 0.5 K. Negative values are shaded.

The effects of air traffic increase and climate change can be separated from each other by performing GCM simulations for both future time slices with and without changes in sea surface temperature and atmospheric composition. Generally, the impact of changes in air traffic (Fig. 3, middle panels) dominates over the effect of climate change (Fig. 3, lower panels). (We use ratios to display changes; thus, the results in the upper panels are yielded as the product of those in the lower two panels.) The relatively strong increase in contrail cover over Southeast Asia and respective flight routes to Europe and the United States is due to especially high future growth rates of aviation in these areas. Local increases by one order of magnitude occur between 1992 and 2050.

Climate change tends to reduce contrail cover, because enhanced greenhouse gas concentrations increase tropospheric temperatures. The most important impact of climate change is found between 30°S and 30°N, where temperature increases up to 5 K occur from 1992 to 2050 at the main flight altitudes [Fig. 4; see also Fig. 11a of Roeckner et al. (1999)]. This warming would lead to local decreases in contrail cover of up to a factor of 5 if air traffic did not increase in the respective time period (Fig. 3, lower right panel). In the midlatitudes, temperature change is more moderate and the effect of climate change on contrail cover is nearly negligible. Although it is not surprising that climate change affects contrail cover preferably in regions where it is most pronounced, it has to be recalled that the temperature sensitivity of contrail formation depends on the absolute temperature regime: the formation of contrails is more sensitive to a given temperature change in the Tropics than in the extratropics, because tropical temperatures tend to be higher and are often close to the threshold temperature for thermodynamic contrail formation at the relevant altitude range (see also section 3b).

On the global scale, changes in air traffic lead to an increase in contrail cover from 0.06% in 1992, to 0.15% in 2015, and to 0.28% in 2050, if climate change is neglected. Note that the values for all three time slices are lower than the ones presented by Gierens et al. (1999), who obtained 0.09% (1992), 0.2% (2015), and 0.5% (2050). This is partly due to a different calibration as explained in section 2, and partly it is related to systematic deviations between the model climate and the observed climate, as will be discussed in section 3b. If future climate change is considered in addition, global mean contrail cover reduces in the model simulations to 0.14% in 2015 and 0.22% in 2050. It can be concluded that the global contribution of climate change to changes in contrail cover is small compared to the contribution of changes in air traffic. Note, however, that the contribution of climate change would be larger if air traffic density was higher in tropical latitudes, where contrail cover is quite sensitive to climate change.

b. Sensitivity to the model bias

In order to quantify how the contrail cover simulated within the framework of the ECHAM4 GCM is affected by systematic errors in the model climate, a couple of offline diagnostic calculations were performed. As described in section 2, basically two meteorological datasets were used: 1) data from ECMWF reanalysis (ERA) and 2) temperature and humidity data from an ECHAM4 climate simulation. Assuming the ERA data to provide ''true'' 3D distributions of temperature and relative humidity for the time slice 1992, the bias in the GCM's climate can be determined as the difference be-

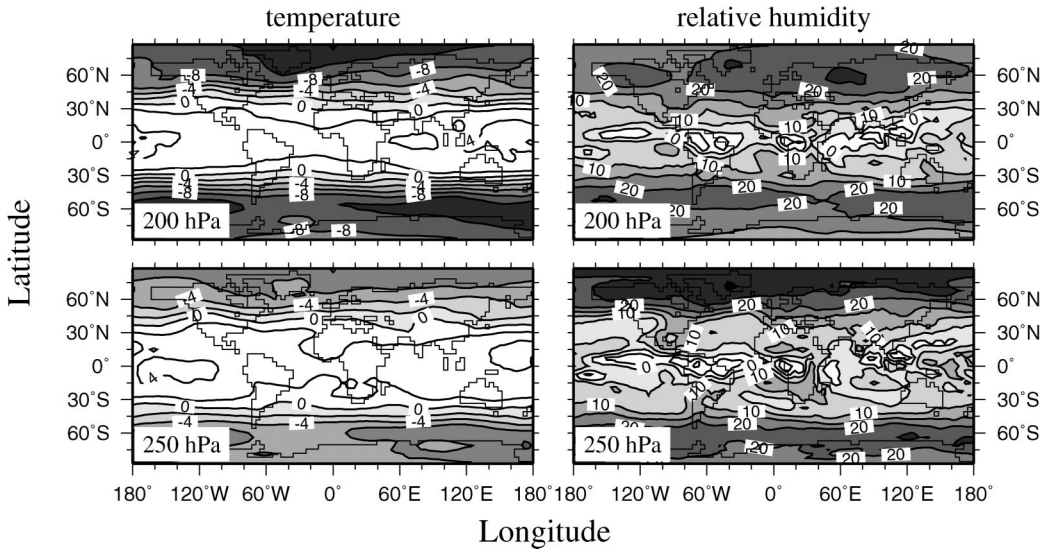

FIG. 5. The 10-yr mean differences of (left) temperature (K) and (right) relative humidity with respect to ice (%) between data from the ECHAM4 transient climate change simulation and ECMWF reanalysis data (ECHAM4 minus ERA) at (top) 200 and (bottom) 250 hPa. Isoline spacing is 2 K or 5%, respectively. Negative temperature and positive humidity values are shaded.

tween climatological ECHAM4 and ERA datasets. Figure 5 shows the bias in atmospheric temperatures and in relative humidities at the 200- and 250-hPa levels, which happen to be not only the altitude range where most aircraft fly, but also the altitude range where the systematic errors in model climate are most pronounced.

As obvious from Fig. 5 (left), the ''cold bias'' of atmospheric temperatures in its typical form (Boer et al. 1992; Gates et al. 1999) is restricted to latitudes poleward of about 40°N and 40°S and shows maximal differences of up to −12 K over Greenland and the Antarctic Sea at 200 hPa. The tropical regions between 30°S and 30°N, on the other hand, are characterized by a ''warm bias'' of up to 5-K-too-high temperatures over the equatorial Pacific Ocean. The bias in temperature is accompanied by a bias in relative humidity (Fig. 5 right). At polar latitudes the model simulates relative humidities higher than observed, because the cold bias leads to a smaller static stability in the upper troposphere and a lifted tropopause (Santer et al. 2003, their Fig. 1). Hence, moist air is allowed to reach higher altitudes. The relative humidity difference yields a maximum of up to 30% over the Arctic at 250 hPa. Outside the polar regions the differences to the observations are smaller but the model keeps to show higher moisture except for few regions in the inner Tropics.

Figure 6 shows how the total contrail coverage is affected by systematic errors in 3D temperature and humidity, while Table 1 gives the regional mean effect for the key areas indicated in Fig. 2. In order to enable a direct comparison between the calculations with ERA and ECHAM4 data, the same calibration factor was used for both diagnostics; that is, the calculations were not calibrated independently. As we regard the ERA data to represent the true climate, we chose the respective calculation as the base case, which was calibrated to the observations by Bakan et al. (1994) as described above. The same calibration factor was also used for all calculations with ECHAM4 data, which are denoted as ''not individually calibrated'' (marked with the superscript ''nc'') in the following. This procedure of shifting the calibration factor from ERA to ECHAM4 data allows us to quantify the effect of the model bias on contrail cover in a most straightforward way. Note, however, that the contrail coverage from calculations that were not individually calibrated should not be used for a comparison with observations.

According to Fig. 6 (top) the contrail coverage diagnosed from GCM data is systematically too high in cold bias regions, which are characterized by too low temperatures and too high relative humidities, while too few contrails form in the tropical warm bias areas. For example, the contrail cover in the Bakan area or the Japan region nearly doubles if ECHAM4 data instead of ERA data are used for contrail diagnostics. In contrast, the coverage in the tropical Thailand region is reduced by a factor of more than 2 (Table 1). Global mean contrail cover increases from 0.07% to 0.10%.

In order to separate the effects of the bias in temperature and the bias in humidity on regional contrail cover, further offline calculations were performed using ''partly corrected'' ECHAM4 climate data. The correction was done by adding the respective 10-yr mean difference between ERA and ECHAM4 gridbox data to the ECHAM4 data. (Note that the simultaneous correction of both temperature and humidity would result in a nearly perfect agreement with the ERA-off calculations.) If only the temperature field is corrected

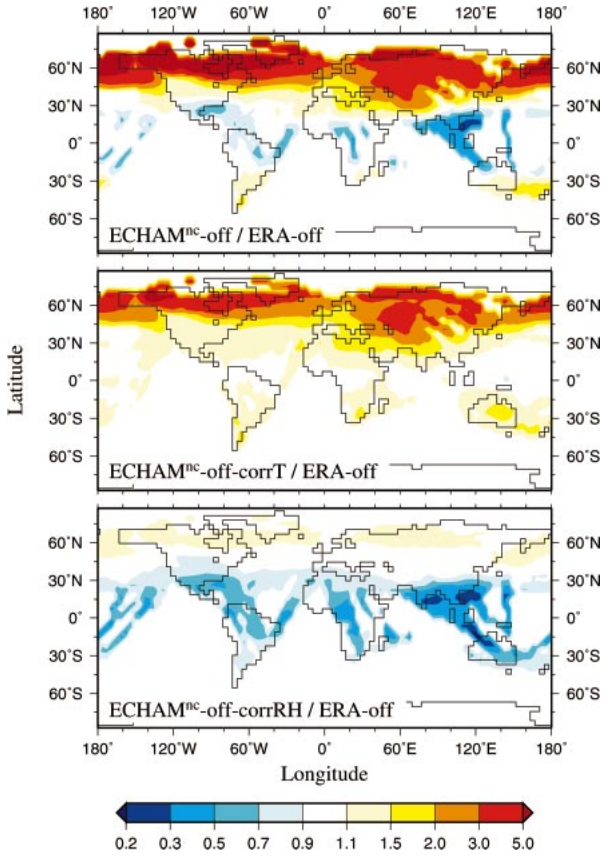

FIG. 6. Ratios of total contrail cover between different offline scenarios for the time slice 1992: (top) ECHAM^{nc}-off/ERA-off; (middle) ECHAM^{nc}-off-corrT/ERA-off; (bottom) ECHAM^{nc}-off-corrRH/ERA-off. Yellow and red signifies a locally higher, blue a locally lower contrail cover compared to ERA data. The same calibration factor was used for all calculations. Calculations not individually calibrated are marked with the superscript ''nc'' (see text).

(ECHAM^{nc}-off-corrT; Table 1; Fig. 6, middle), contrail cover is reduced in the northern extratropics (Bakan, western Europe, Japan) compared to the study with uncorrected ECHAM4 data (ECHAM^{nc}-off) but is still significantly higher compared to the ERA-off calulation. For the United States, which is to the northern part located in the cold bias region, to the southern part in the warm bias region, the temperature correction alone even leads to a worse agreement with the ERA-off calculation. In the tropical regions, the temperature correction alone causes a thorough improvement, with contrail coverage differing only slightly from the ERA-off calculations.

The correction of the relative humidity fields only (ECHAM^{nc}-off-corrRH; Table 1; Fig. 6, bottom) has quite different consequences for contrail cover than the pure temperature correction. Interestingly, the correction of the humidity distribution leads to a nearly perfect agreement with the results of the ERA-off calculation in the northern extratropics (Bakan, western Europe, Japan), although these regions suffer most from the

TABLE 1. Annually averaged total contrail cover (%) in 1992 for different regions. The regions are those marked in Fig. 2. The columns refer to results from offline calculations using different meteorological data: ECMWF reanalysis data (ERA-off), ECHAM4 climate model data (ECHAM^{nc}-off), and ECHAM4 climate model data with a corrected temperature (ECHAM^{nc}-off-corrT) or humidity distribution (ECHAM^{nc}-off-corrRH). The same calibration factor was used for all calculations. Calculations not individually calibrated are marked with the superscript ''nc.'' Calibration is shown in bold.

Region	ERA-off	ECHAM^{nc}-off	ECHAM^{nc}-off-corrT	ECHAM^{nc}-off-corrRH
World	0.07	0.10	0.10	0.05
Bakan	**0.37**	0.71	0.62	0.37
Western Europe	0.88	1.53	1.39	0.87
United States	0.75	0.92	0.96	0.61
Japan	0.18	0.34	0.27	0.17
Thailand	0.12	0.05	0.13	0.04

GCM's temperature bias. Obviously, the correct capture of the observed temperature is much less crucial for contrail formation in these regions than relative humidity, implying that most of the time the ambient air is cold enough for contrail formation anyway. In the tropical regions, the humidity correction alone tends to worsen the agreement with the ERA-off calculations, especially in regions that are characterized by a ''moist bias'' in the GCM.

To sum up the general results of the sensitivity studies, the impact of systematic errors in the model climate must be regarded as qualitatively and quantitatively distinctive for different regions. While the contrail cover in the northern extratropics is only slightly affected by the literal cold bias, it reacts very sensitively to the associated bias in relative humidity. The opposite is true for the contrail cover between 30°S and 30°N, where the correction of the temperature fields is of much greater importance than the humidity correction. Interestingly, the tropical warm bias has a much greater direct importance for contrail cover calculations than the much more pronounced extratropical cold bias. For regions like the United States, which include both cold bias and warm bias contributions, the correction of only one parameter is completely unsuitable to achieve better agreement with ERA-based calculations. Therefore, a selective online temperature correction by a relaxation or nudging technique (e.g., Feichter and Lohmann 1999) will not necessarily lead to a substantial improvement of the GCM simulated contrail coverage.

c. Effect of the model bias on the GCM results

In Table 2 results of the GCM simulations and offline calculations are compared for all regions and time slices considered. The results for the time slices 2015 and 2050 include both changes in air traffic and changes of climate in all studies. In contrast to the sensitivity tests described in the last section (Fig. 6 and Table 1), the GCM simulations and the offline diagnostics for 1992 had to be calibrated individually to achieve a fair comparison of

TABLE 2. Annually averaged total contrail cover (%) for different time slices and different regions. The regions are those marked in Fig. 2. The columns refer to results from online simulations (-on) and offline calculations (-off) using different meteorological data: ECHAM4 climate model data (ECHAM), ECMWF reanalysis data (ERA), and ECHAM4 climate model data that were ''corrected'' by the mean difference of both temperature and humidity fields between ECHAM and ERA data in 1992 (ECHAM-corr). Each model is calibrated individually to contrail observations by Bakan et al. (1994). The values in parentheses are obtained by neglecting the visibility threshold for the model calibration. Calibration is shown in bold.

Year	Region	ERA-off	ECHAM-off	ECHAM-on
1992	World	0.07	0.05	0.06 (0.05)
	Bakan	**0.37**	**0.37**	**0.37 (0.37)**
	Western Europe	0.88	0.80	0.83 (0.82)
	United States	0.75	0.48	0.61 (0.46)
	Japan	0.18	0.18	0.17 (0.12)
	Thailand	0.12	0.02	0.06 (0.04)
		ECHAM-off-corr	ECHAM-off	ECHAM-on
2015	World	0.15	0.12	0.14
	Bakan	0.79	0.81	0.88
	Western Europe	1.75	1.72	1.97
	United States	1.50	0.96	1.17
	Japan	0.68	0.57	0.58
	Thailand	0.39	0.08	0.24
2050	World	0.28	0.22	0.22
	Bakan	1.49	1.44	1.52
	Western Europe	3.01	2.90	3.12
	United States	1.79	1.25	1.28
	Japan	1.19	0.94	0.92
	Thailand	0.72	0.13	0.27

the different methods. Hence, in all calculations discussed for the rest of this section contrail coverage was calibrated to 0.37% in the Bakan area for the time slice 1992.

The investigation of the effect of the bias in the ECHAM4 model climate is less straightforward for future scenarios than it is for the recent 1992 scenario, because observations are lacking for future time slices. Hence, we assume that the bias in the GCM's climate is sufficiently constant throughout the years and perform offline calculations with ''corrected'' ECHAM data: ECHAM4 temperature and humidity fields for the time slices 2015 and 2050 are corrected by 10-yr mean differences between ECHAM4 and ERA data in 1992 (ECHAM-off-corr). This should be sufficient for an impression of how the impact of model errors may influence results for future climates.

If one compares the calculations ERA-off and ECHAM-off (or ECHAM^{nc}-off, respectively) for the time slice 1992 in Tables 1 and 2, the effect of the individual calibration of the calculation using ECHAM4 data becomes obvious. As the contrail coverage is now forced to a value of 0.37% in the Bakan area, the error in contrail cover resulting from too high relative humidity there is shifted to regions outside the calibration area. Therefore, the new calibration improves the results for contrail cover in the northern extratropics, where contrail cover had been too high, but at the same time worsens them in tropical regions, where contrail cover had been too low anyway. In these regions, for example, over the Thailand region, the contrail cover gets severely underestimated, partly because of the local temperature bias, partly because of the artificial ''error transfer'' from the calibration area.

The 1992 contrail coverage computed within the GCM framework (ECHAM-on) is somewhere in between the results of the two offline calculations (Table 2) for most regions; that is, the agreement with the true ERA-off coverage is better in most cases than in the ECHAM-off study. Note especially the three-times-higher contrail cover over the Thailand region. Differences between the ECHAM-off and ECHAM-on estimations arise, as mentioned before, mainly from a more sophisticated model setup regarding criteria of contrail persistence, a higher vertical resolution, and the calibration threshold in the online model. If the threshold optical depth for calibration is neglected, that is, set to zero (instead of 0.02), contrail coverage decreases within regions whose mean optical depth is higher than in the calibration area (as less contrails fall below a optical depth of 0.02 in those regions). The results from a thus modified GCM parameterization come quite close to the results of the ECHAM-off calculation (Table 2, values in parentheses).

Considering the future scenarios, the comparison of the results from different calculation methods gives similar conclusions as for the 1992 time slice. The agreement with the ''true'' ECHAM-off-corr calculation remains quite good in or near the calibration area (Bakan, western Europe), implying that the relative change in contrail cover due to climate change can be regarded to be quite independent from the bias in model climate. Relative to the ERA-off or the ECHAM-off-corr calculations, respectively, the online simulations tend to underestimate contrail coverage over Japan (factor of 0.8–0.9), the United States (factor of 0.7–0.8), Thailand (factor of 0.4–0.6), and in the global mean (factor of 0.8–0.9). There is no obvious trend in these numbers from 1992 to 2050, meaning that the systematic errors in the model climate seem to induce a similar relative change in contrail cover throughout the different time slices and underlying climates. Apparently, the temperature change between 1992 and 2050 is too small to induce significant nonlinear effects. This is, of course, very convenient for interpreting the result of the online contrail simulations.

The quantitative results presented here, that is, the underestimation of contrail cover by the GCM simulations in most regions of the world, crucially depend on the choice of the calibration area. If the model calibration was done, for example, in the Thailand region instead of the Bakan region, this would lead to an excellent agreement of contrail cover in tropical regions,

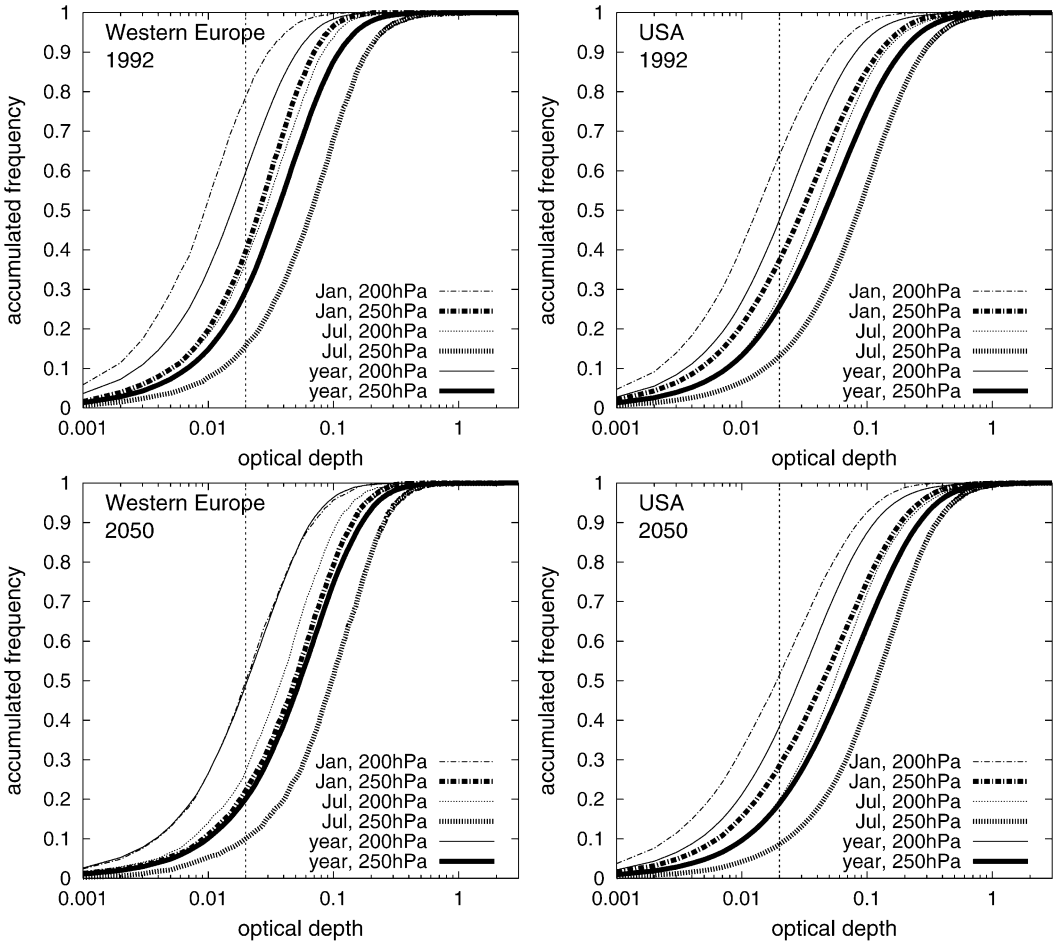

FIG. 7. Distribution functions of the contrail optical depth simulated by ECHAM4 for the time slices (top) 1992 and (bottom) 2050 over (left) western Europe and (right) the United States, for different seasons (annual mean, Jan, Jul) and altitudes (200 and 250 hPa). See Fig. 2 for the definition of the regions. The threshold optical depth of 0.02 is marked by the vertical dotted line.

whereas coverage in the midlatitudes would be substantially overestimated.

In general, the results of this section should primarily be understood as indicative. Quantitative conclusions would imply the ''truth'' of the ERA climate mean data and the related ERA-off calculation, which may well contain its own deficiencies, too. First, as pointed out before, the offline diagnostic tool has to be regarded as conceptually inferior to the online model mainly because contrail persistence cannot be accounted for. Second, the meteorological ERA data may contain systematic errors especially regarding the relative humidity distribution in the upper troposphere and lower stratosphere, as the water vapor content in this altitude range is still considerably uncertain from the point of view of observation quality (Peixoto and Oort 1996; Ovarlez et al. 2000).

4. Optical depth

As the radiative impact of contrails does not only depend on coverage, but also on their optical properties, it is worthwhile to look at the temporal development of the contrail optical depth in a changing climate. Ponater et al. (2002) have already discussed the general features of contrail optical depth for the 1992 climate conditions, simulated within the framework of the ECHAM4 GCM. They found increasing optical depth from higher to lower altitudes, from the poles toward the equator, and from winter to summer. Mean values for ice water content and optical depth were found to be consistent with, but rather on the lower end of, measurements in contrails (e.g., Gayet et al. 1996; Betancor Gothe et al. 1999; Schröder et al. 2000).

Figure 7 shows distribution functions of the optical depth over western Europe and the United States for different altitudes (200 and 250 hPa), seasons (January, July, annual mean), and time slices (1992, 2050). The individual optical depth values prove to be highly variable not only between different locations, but also from time step to time step in a given region, covering the wide range of local observations (Gayet et al. 1996; Sassen 1997; Jäger et al. 1998; Betancor Gothe et al.

TABLE 3. Annually and globally averaged total contrail cover and radiative forcing components, as well as global annual fuel consumption in 1992, 2015, and 2050. Values in parentheses are adjusted by a 25% offset to the longwave contrail radiative forcing (see text). Changes in air traffic, propulsion efficiency (η), and climate are taken into account. Bold entries indicate the most likely scenario for the respective time slice.

Year	Fuel (Tg yr^{-1})	η	Climate change	Cover (%)	Radiative forcing (mW m^{-2})		
					Longwave	Shortwave	Net
1992	112	**0.3**	—	**0.06**	3.7 (**4.9**)	**−1.4**	2.3 (**3.5**)
2015	271	0.3	No	0.13	8.6 (11.5)	−3.1	5.5 (8.4)
		0.4	No	0.15	10.1 (13.5)	−3.7	6.4 (9.8)
		0.4	**Yes**	**0.14**	9.8 (**13.1**)	**−3.7**	6.1 (**9.4**)
2050	471	0.3	No	0.23	14.7 (19.6)	−5.3	9.4 (14.3)
		0.5	No	0.28	20.2 (26.9)	−7.4	12.8 (19.5)
		0.5	**Yes**	**0.22**	15.5 (**20.7**)	**−5.9**	9.6 (**14.8**)

1999; Minnis et al. 1999; Meyer et al. 2002b). Consistent with apparent differences in observed contrail optical depth over Europe and the United States (Minnis et al. 1999; Meyer et al. 2002b), optically thicker contrails are simulated over the United States than over western Europe. The distribution functions for both regions show considerable differences with respect to altitude and season. For example, over western Europe the fraction of contrails with optical depth values ranging below the visibility threshold of 0.02 amounts to nearly 0.8 in the 200-hPa level for 1992 January conditions, but only to about 0.15 in the 250-hPa level for July conditions (Fig. 7 top left).

Comparing the distribution functions for the time slices 1992 and 2050 reveals that the optical depth tends to increase in a warming climate. Rising temperatures will generally increase the atmospheric water vapor amount available for condensation, leading to a potentially higher ice water content within contrails and therefore a higher mean optical depth. For instance, the annual mean fraction of nonvisible contrails decreases in 250 hPa in western Europe from about 0.3 in 1992 to 0.2 in 2050 (Fig. 7, left). Note that in this region, the distribution function for January 2050 and the annual mean 2050 come quite close (Fig. 7, bottom left), while the distribution function tends to shift toward lower optical depth in early spring (not shown). On the global scale, optical depth increases by a factor of about 1.2 from 1992 to 2050 (not shown).

As optical depth depends on temperature it is obvious that it may also be affected by systematic errors in the modeled temperature distribution. The structure of the temperature bias in ECHAM4 (Fig. 5) suggests a slight overestimation of optical depth values in the tropical warm bias regions, but especially a much more severe underestimation in the cold bias regions north of about 45°N. Therefore, the cold bias may be a possible explanation for the relatively high fraction of low optical depth values simulated in the northern extratropics, for example, for western Europe.

5. Radiative forcing

a. Recent conditions and future projections

Future changes in radiative forcing of contrails result, on the one hand, directly from changes in the atmospheric environment, on the other hand, indirectly from changes in contrail cover and optical depth. In Table 3, the global annual mean radiative forcing is listed for all GCM simulations considered, along with the respective annually averaged contrail cover and the total annual fuel consumption. For these radiative forcing calculations, which follow the lines described in Ponater et al. (2002) and the amendments of Marquart and Mayer (2002), nonspherical ice particles with an ice water–dependent effective radius (ranging mostly between 12 and 13 μm) are assumed. Marquart and Mayer (2002) report that the global mean longwave forcing from contrails is still systematically underestimated by the upgraded ECHAM4 radiative transfer scheme due to the exclusion of longwave scattering. Therefore, we also present radiative forcing values, which were corrected a posteriori for the respective 25% offset (Table 3, numbers in parentheses). These ''adjusted'' values should be regarded as our best estimate for the contrail radiative forcing from the GCM simulations.

Considering changes in air traffic, propulsion efficiency, and climate, contrail net radiative forcing increases from 2.3 (3.5) mW m^{-2} in 1992 to 6.1 (9.4) mW m^{-2} in 2015, and to 9.6 (14.8) mW m^{-2} in 2050; that is, the radiative impact of contrails increases by more than a factor of 4 from 1992 to 2050 (Table 3). If only changes in air traffic density are considered, the net radiative forcing depends quite linearly on the aviation fuel consumption (Fig. 8, right). In contrast, a slight saturation effect appears for total contrail cover (Fig. 8, left), which is due to the maximum-overlap assumption for the vertical integration of 3D contrail cover. Growing propulsion efficiency leads to increases in contrail cover and radiative forcing, while climate change tends to reduce them. If climate change is taken into account, the net radiative forcing is reduced by about 25% in 2050 with respect to the scenario where

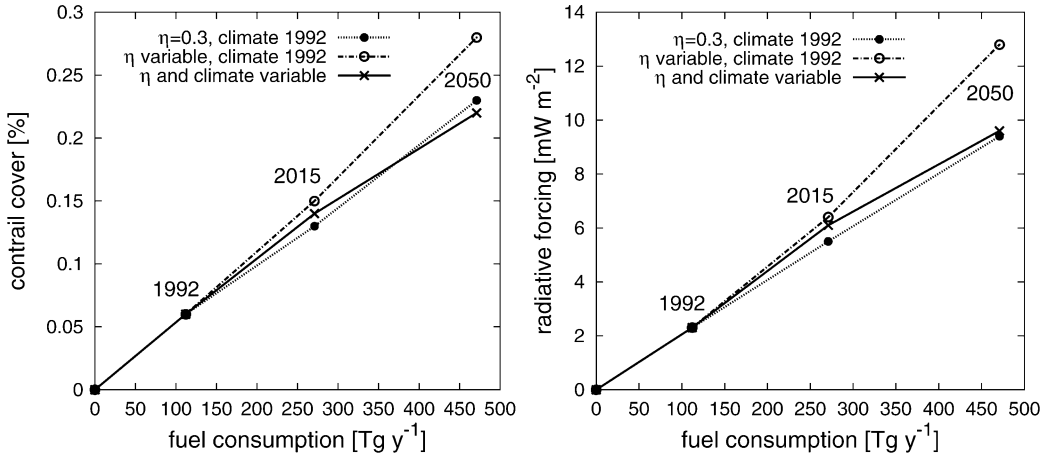

FIG. 8. (left) Anually and globally averaged total contrail cover and (right) net radiative forcing in 1992, 2015, and 2050, displayed as a function of global annual fuel consumption. Changes in air traffic, propulsion efficiency (η), and climate are taken into account.

climate change is neglected (Table 3). By coincidence, the increases due to a greater propulsion efficiency are nearly cancelled by the effects of climate change in 2050 (Fig. 8 and Table 3). Note that the damping influence of climate change is less apparent for radiative forcing than it is for contrail coverage. Here, the influence of an increasing contrail optical depth in the future scenarios becomes obvious.

Eventually, for further increases in air traffic, radiative forcing will begin to show saturation effects. However, a model study assuming 10 times the fuel consumption of 2050 does not yet result in a significant deviation from linearity (not shown). Therefore, the radiative impact of contrails is not likely to come close to saturation during the forthcoming decades.

The 1992 estimate for net radiative forcing that we deduce from the GCM simulations of 3.5 mW m^{-2} is lower by a factor of 5 than the 17 mW m^{-2} provided as a best estimate by Penner et al. (1999). This discrepancy can be attributed mainly to differences in contrail cover (due to different calibration) and especially optical depth, as the IPCC estimate relies on contrail coverage provided by Sausen et al. (1998) and a fixed optical depth of 0.3. The same factor of 5 occurs for the time slice 2050 between the IPCC's best estimate of 100 mW m^{-2} and our GCM simulation if climate change is neglected, as was done by IPCC.

b. Sensitivity considerations

Besides coverage and ice water content, model estimates for global mean radiative forcing depend on several more factors such as assumptions about microphysical particle properties, or the treatment of the interference of contrails with natural cirrus. For example, in the extreme scenario of a ''clear-sky'' atmospheric environment, where apart from contrails no clouds are allowed, both a larger longwave and shortwave contrail radiative impact is induced because both the greenhouse and the albedo effect of contrails increase. In a clear-sky GCM simulation, the increase of shortwave radiative forcing (by about 60%) is stronger than the increase of longwave radiative forcing (by about 25%), resulting in a global annual mean net radiative forcing that is enhanced by only 10%. Less extreme assumptions, such as an idealized overlap of the modeled contrails with natural clouds, should affect contrail radiative forcing even less.

Spherical particles induce a weaker shortwave radiative forcing and therefore a stronger net radiative forcing than nonspherical particles (Meerkötter et al. 1999; Zhang et al. 1999). If we assume contrail particles to be of spherical shape in our simulations, the annually averaged global net radiative forcing is 2.8 (4.0) W m^{-2} for 1992, that is, 15%–20% higher than in our reference simulation (Table 3).

However, not only the shape, but also the size of contrail particles, is presently a matter of uncertainty. In order to quantify this, a number of GCM simulations were performed for different effective radii of contrail particles. As expected from previous studies (Fu and Liou 1993; Meerkötter et al. 1999; Zhang et al. 1999), a decrease in both longwave and shortwave radiative forcing with increasing particle size is found (Fig. 9). However, the net radiative forcing shows a maximum around 9–12 μm because the shortwave albedo effect increases more strongly than its longwave counterpart toward small effective radii beyond 9 μm. This nonlinear relationship between net radiative forcing and the effective ice crystal radius was mentioned before by, for example, Fu and Liou (1993), Fortuin et al. (1995), Meerkötter et al. (1999), and Zhang et al. (1999). These studies pointed out the possibility of a negative net forcing of cirrus clouds if they contain small particles. However, this would also require ice water contents that are much higher as those generally found in persistent con-

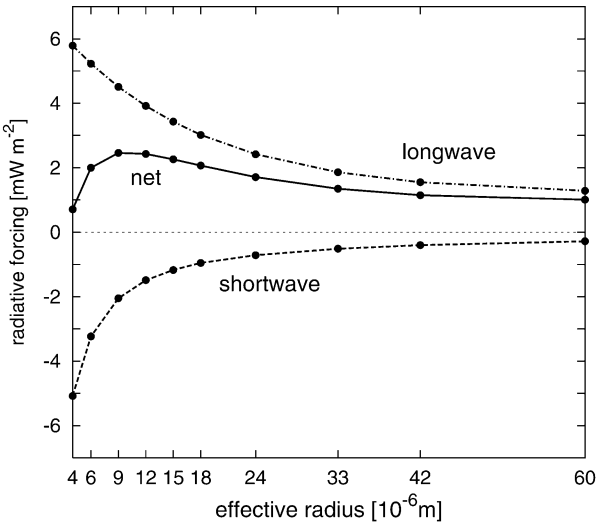

FIG. 9. Annually and globally averaged radiative forcing (longwave, shortwave, net) of contrails dependent on the effective particle radius. Every dot denotes the result of a 2-yr model simulation. The ice water content is as simulated by the GCM for 1992 conditions.

trails. For a higher mean ice water path the maximum in contrail net forcing (Fig. 9) shifts toward larger effective radii (not shown).

In our reference simulations the parameterized effective radii of contrail particles mostly range in a quite narrow band around 12–13 μm. Taken as a mean value this compares reasonably well to observed particle sizes (see Schumann 2002, and references therein). As this value is close to that for which the net radiative impact is at its maximum, substantial decreases and increases of the particle size both would tend to decrease radiative forcing. For example, either half or double mean effective radii lead to a 15% or 25% lower net contrail forcing, respectively. This finding involves a further, somewhat hidden, sensitivity of the radiative forcing, which we estimate: even if a quantity such as a ''typical'' or ''mean'' particle size was exactly known, using this value instead of the underlying particle size distribution for radiative transfer calculations would induce a systematically too large contrail radiative forcing in cases where the size distribution around the mean covers a wide range.

According to previous studies, the occurrence of line-shaped contrails closely follows the daily variations of aviation in the respective region (Meyer et al. 2002a,b). The corresponding diurnal cycle of contrail radiative forcing is not so straightforward, because shortwave radiative forcing additionally depends on the solar zenith angle. For a given contrail coverage, the strongest shortwave radiative impact (and therefore the weakest net radiative forcing) occurs at high zenith angles near sunrise or sunset, while it is zero during nighttime and shows a minimum during day at noon (Meerkötter et al. 1999). While the diurnal variation of local contrail radiative forcing strongly depends on the daily cycle of air traffic in the respective region, this is much less obvious for the global and annual mean scale. In order to quantify this effect, we included the diurnal cycle in a GCM simulation for the 1992 air traffic (Schmitt and Brunner 1997). The result was a decrease of global annual mean net radiative forcing by less than 10% compared to our reference 1992 simulation, where the daily cycle of air traffic is neglected. Hence, it appears that the impact of the daily cycle of air traffic on the globally and long-term averaged contrail radiative forcing is small compared to other uncertainties regarding contrail radiative forcing. This is in some disagreement with previous studies, which regarded the daily cycle of air traffic as a quite important sensitivity parameter for global mean radiative forcing (Mannstein et al. 1999; Myhre and Stordal 2001). However, these studies were based on regional findings, where radiative forcing may indeed strongly depend on air traffic characteristics. For example, for western Europe or Japan, global annual mean net radiative forcing is overestimated by nearly 30% in our simulations if the diurnal variation of air traffic is neglected.

6. Conclusions and outlook

The future development of line-shaped contrails was investigated considering changes in air traffic, aircraft technology, as well as climate change. We made use of the contrail parameterization for the ECHAM4 GCM following Ponater et al. (2002) and including the amendments by Marquart and Mayer (2002), which allows us to simulate contrail coverage, optical depth, and radiative forcing self-consistently within a unified model framework. Furthermore, we performed offline diagnostic studies in order to quantify the impact of the GCM's systematic temperature and humidity errors on which contrail formation and coverage crucially depend.

Time slice GCM simulations for 1992, 2015, and 2050 show an increase in global annual mean contrail cover from 0.06% in 1992, to 0.14% in 2015, and to 0.22% in 2050 (Fig. 10, ECHAM-on, diagonal axis). If climate change is neglected, contrail cover increases more strongly to 0.15% in 2015 and to 0.28% in 2050 (Fig. 10, ECHAM-on, first row). Nevertheless, the damping effect of climate change on global contrail cover is dominated by the effect of the proposed increase in air traffic.

In the northern extratropics, where most air traffic occurs, future temperature change predicted in climate model simulations is moderate in the upper troposphere and the lower stratosphere. Therefore, the future enhancement of contrail cover is mainly determined by the growth of aviation in these regions. In the Tropics, however, the future development of contrail cover does not only depend on the (considerable) increase of air traffic, but is also highly affected by climate change, which is expected to be most pronounced in these latitudes. Moreover, contrail formation is more sensitive

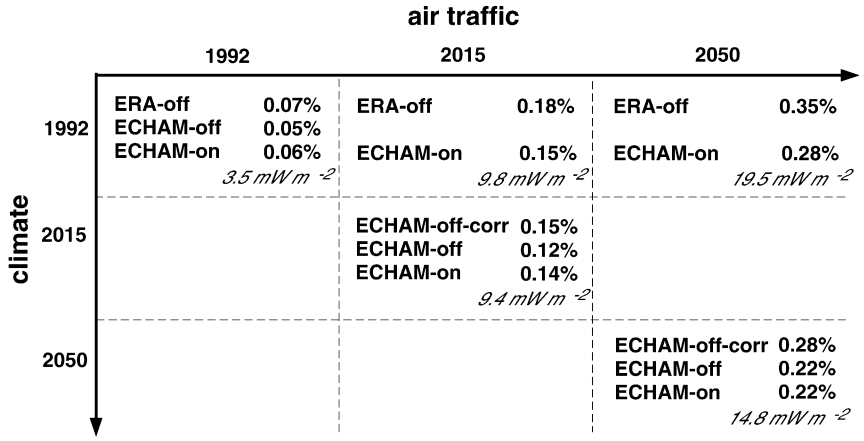

FIG. 10. As in Fig. 1, but including results for global annual mean contrail cover and radiative forcing. Values in the first row (ERA-off, climate 1992) are the same as in Gierens et al. (1999) scaled with a factor of 0.75 due to the different calibration method used in the present paper.

to temperature fluctuations in the tropical regions than in the midlatitudes. In some equatorial regions, the climate change between 2050 and 1992 would lead to a reduction in local contrail cover by up to a factor of 5, if air traffic did not increase in the respective time period.

Offline contrail diagnostics with ECMWF reanalysis (ERA-off) and ''bias-corrected'' ECHAM meteorological data (ECHAM-off-corr) suggest a systematic underestimation of global mean total contrail cover in the GCM simulations by a factor of about 0.8–0.9, the relative error being quite independent of the time slice considered. By coincidence, the uncertainty in global contrail cover due to systematic errors in the ECHAM4 model climate is of similar magnitude as the effect due to the proposed temporal change in climate.

In the northern extratropics, the effect of the bias in model climate is small, as contrail cover is calibrated to observations in northern latitudes. However, potential errors in extratropical contrail cover (mainly induced by errors in the relative humidity), which are avoided due to the calibration procedure, are shifted toward tropical regions. This ''error transfer'' adds to the bias due to systematic local temperature errors, which have a comparatively high potential to affect contrail cover in the Tropics. Altogether, tropical contrail cover is underestimated by roughly a factor of 2 in the GCM simulations.

The future development of the contrail radiative forcing is mainly determined by the total contrail cover, although the mean optical depth is found to increase in a warmer climate, too. Our best estimate from the GCM simulations is an increase of global annual mean radiative forcing from 3.5 mW m^{-2} in 1992, to 9.4 mW m^{-2} in 2015, and to 14.8 mW m^{-2} in 2050, if both changes in air traffic and climate are considered (Fig. 10, ECHAM-on, diagonal axis). The values for 2015 and 2050 change to 9.8 and 19.5 mW m^{-2}, respectively, if climate change is neglected (Fig. 10, ECHAM-on, first row). If only changes in air traffic density are considered, global mean radiative forcing is found to grow approximately linearly with fuel consumption far beyond 2050.

The deviation from the best estimate for global contrail radiative forcing provided by Penner et al. (1999), which is about a factor of 5 higher than our results, is mainly due to their simpler assumptions regarding contrail cover and, especially, optical depth. Further uncertainties arise from insufficient knowledge about particle shapes and sizes. Altogether, uncertainties in contrail radiative forcing due to insufficient knowledge about contrail microphysics seem to exceed uncertainties arising from inherent model simplifications, such as an idealized treatment of natural clouds or the negligence of the daily cycle of air traffic.

Finally, we would like to recall that the present study deals with the climate impact of line-shaped contrails, while the overall effect of aviation-induced changes in cirrus cloudiness may be much larger (Boucher 1999). In this context we note that in the present study radiative or other feedbacks of the contrails themselves on the global climate have not been included. As contrails produce a positive radiative forcing, they are expected to contribute to global warming. Increasing temperatures tend to induce decreasing contrail cover, leading consequently to a reduced global warming due to contrails. The existence of such a negative feedback loop could and should be investigated by means of GCM studies that allow not only for the climate to affect contrail formation, as was done in the present studies, but also for contrails to affect climate. Apart from the direct radiative feedback between contrails and climate, there is another possible feedback due to the transition of linear contrails to nonlinear cirruslike clouds. Our model framework offers the possibility to include such a contrail-to-cirrus transition by adding the ice water formed within contrails to the total cloud ice when contrails

lose their linear shape. Adding this feedback to the direct radiative feedback would probably enhance the climate impact of contrails substantially (Minnis et al. 1998; Schumann 2002). Climate simulations that include feedbacks between contrails and climate would also allow us to determine a special climate sensitivity parameter (i.e., the ratio between global mean surface temperature change and radiative forcing) for line-shaped contrails, similar to the special climate sensitivity parameter deduced by Stuber et al. (2001a) for localized ozone perturbations.

Acknowledgments. The authors are grateful to K. Gierens, S. Uppala, and P. Kallberg for helpful discussions. Parts of this work were funded by the EU projects ''TRADEOFF'' and ''SCENIC.'' The first author has received support from the ''Studienstiftung des deutschen Volkes.''

REFERENCES

Bakan, S., M. Betancor, V. Gayler, and H. Graßl, 1994: Contrail frequency over Europe from NOAA-satellite images. *Ann. Geophys.,* **12,** 962–968.

Baughcum, S. L., D. J. Sutkus, and S. C. Henderson, 1998: Year 2015 aircraft emission scenario for scheduled air traffic. Tech. Rep. CR-1998-207638, NASA Langley Research Center, Hampton, VA, 44 pp.

Betancor Gothe, M., M. Dreyer, S. Bakan, and C. Costanzo, 1999: Ground based passive remote sensing of ice clouds with scattered solar radiation in the near infrared. *Phys. Chem. Earth,* **24B,** 219–224.

Boer, G., and Coauthors, 1992: Some results from an intercomparison of the climates simulated by 14 general circulation models. *J. Geophys. Res.,* **97,** 12 771–12 786.

Boucher, O., 1999: Air traffic may increase cirrus cloudiness. *Nature,* **397,** 30–31.

Feichter, J., and U. Lohmann, 1999: Can a relaxation technique be used to validate clouds and sulphur species in a GCM? *Quart. J. Roy. Meteor. Soc.,* **125,** 1277–1294.

Fortuin, J. P. F., R. van Dorland, W. M. F. Wauben, and H. Kelder, 1995: Greenhouse effects of aircraft emissions as calculated by a radiative transfer model. *Ann. Geophys.,* **13,** 413–418.

Fu, Q., and K. N. Liou, 1993: Parameterization of the radiative properties of cirrus clouds. *J. Atmos. Sci.,* **50,** 2008–2025.

Gates, W. L., and Coauthors, 1999: An overview of the results of the Atmospheric Model Intercomparison Project (AMIP I). *Bull. Amer. Meteor. Soc.,* **80,** 29–55.

Gayet, J.-F., G. Febvre, G. Brogniez, H. Chepfer, W. Renger, and P. Wendling, 1996: Microphysical and optical properties of cirrus and contrails: Cloud field study on 13 October 1989. *J. Atmos. Sci.,* **53,** 126–138.

Geleyn, J. F., and A. Hollingsworth, 1978: An economical analytical method for the computation of the interaction between scattering and line absorption of radiation. *Beitr. Phys. Atmos.,* **52,** 1–16.

Gibson, J. K., P. Kallberg, S. Uppala, A. Hernandez, A. Nomura, and E. Serrano, 1997: ERA description. ECMWF Re-Analysis Project Report Series, Vol. 1, 1–72.

Gierens, K., R. Sausen, and U. Schumann, 1999: A diagnostic study of the global distribution of contrails. Part II: Future air traffic scenarios. *Theor. Appl. Climatol.,* **63,** 1–9.

Houghton, J. T., B. A. Callender, and S. K. Varney, Eds., 1992: *Climate Change 1992—The Supplementary Report to the IPCC Scientific Assessment.* Cambridge University Press, 200 pp.

——, Y. Ding, D. J. Griggs, M. Noguer, P. J. van der Linden, and D. Xiaosu, Eds., 2001: *Climate Change 2001: The Scientific Basis.* Cambridge University Press, 881 pp.

Jäger, H., V. Freudenthaler, and F. Homburg, 1998: Remote sensing of optical depth of aerosols and cloud over related to air traffic. *Atmos. Environ.,* **32,** 3123–3127.

Land, C., M. Ponater, R. Sausen, and E. Roeckner, 1999: The ECHAM4. L39(DLR) atmosphere GCM: Technical description and model climatology. Forschungsbericht 1991-31, Deutsches Zentrum für Luft- und Raumfahrt e.V. (DLR), Cologne, Germany, 45 pp. [ISSN 1434-8454.]

——, J. Feichter, and R. Sausen, 2002: Impact of the vertical resolution on the transport of passive tracers in the ECHAM4 model. *Tellus,* **54B,** 344–360.

Mannstein, H., R. Meyer, and P. Wendling, 1999: Operational detection of contrails from NOAA-AVHRR-data. *Int. J. Remote Sens.,* **20,** 1641–1660.

Marquart, S., and B. Mayer, 2002: Towards a reliable GCM estimation of contrail radiative forcing. *Geophys. Res. Lett.,* **29,** 1179, doi: 10.1029/2001GL014075.

Meerkötter, R., U. Schumann, D. R. Doelling, P. Minnis, T. Nakajima, and Y. Tsushima, 1999: Radiative forcing by contrails. *Ann. Geophys.,* **17,** 1080–1094.

Meyer, R., R. Büll, C. Leiter, H. Mannstein, S. Marquart, T. Oki, and P. Wendling, 2002a: Contrail observations over southern and eastern Asia in NOAA/AVHRR data and intercomparison to contrail simulations in a GCM. DLR Rep. 176, Institut für Physik der Atmosphäre, DLR Oberpfaffenhofen, Germany, 16 pp.

——, H. Mannstein, R. Meerkötter, U. Schumann, and P. Wendling, 2002b: Regional radiative forcing by line-shaped contrails derived from satellite data. *J. Geophys. Res.,* **107** (D10), 4104, doi: 10.1029/2001JD000426.

Minnis, P., D. F. Young, D. P. Garber, L. Nguyen, W. L. Smith Jr., and R. Palikonda, 1998: Transformation of contrails into cirrus during SUCCESS. *Geophys. Res. Lett.,* **25,** 1157–1160.

——, U. Schumann, D. R. Doelling, K. Gierens, and D. W. Fahey, 1999: Global distribution of contrail radiative forcing. *Geophys. Res. Lett.,* **26,** 1853–1856.

——, R. Palikonda, J. K. Ayers, D. P. Duda, and K. P. Costulis, 2000: Cirrus, contrails, and radiative forcing over the USA: Their relationship to air traffic and upper troposphere conditions. *Proc. Conf. on Aviation, Aerosols, Contrails and Cirrus Clouds (A^2C^3),* Seeheim, Germany, European Commission, 193–196.

Myhre, G., and F. Stordal, 2001: On the tradeoff of the solar and thermal infrared radiative impact of contrails. *Geophys. Res. Lett.,* **28,** 3119–3122.

Ovarlez, J., P. van Velthoven, G. Sachse, S. Vay, H. Schlager, and H. Ovarlez, 2000: Comparison of water vapor measurements from POLINAT 2 with ECMWF analyses in high-humidity conditions. *J. Geophys. Res.,* **105,** 3737–3744.

Peixoto, J. P., and A. H. Oort, 1996: The climatology of relative humidity in the atmosphere. *J. Climate,* **9,** 3443–3463.

Penner, J. E., D. H. Lister, D. J. Griggs, D. J. Dokken, and M. McFarland, Eds., 1999: *Aviation and the Global Atmosphere.* Cambridge University Press, 365 pp.

Ponater, M., S. Marquart, and R. Sausen, 2002: Contrails in a comprehensive global climate model: Parameterisation and radiative forcing results. *J. Geophys. Res.,* **107** (D13), 4164, doi:10.1029/2001JD000429.

Roeckner, E., and Coauthors, 1996: The atmospheric general circulation model ECHAM-4: Model description and simulation of present-day climate. Rep. 218, Max-Planck-Institut für Meteorologie, Hamburg, Germany, 90 pp.

——, L. Bengtsson, J. Feichter, J. Lelieveld, and H. Rodhe, 1999: Transient climate change simulations with a coupled atmosphere–ocean GCM including the tropospheric sulfur cycle. *J. Climate,* **12,** 3004–3032.

Santer, B. D., and Coauthors, 2003: Behavior of tropopause height and atmospheric temperature in models, reanalyses, and observations. Part I: Decadal changes. *J. Geophys. Res.,* **108** (D1), 4002, doi:10.1029/2002JD002258.

Sassen, K., 1997: Contrail-cirrus and their potential for climate change. *Bull. Amer. Meteor. Soc.*, **78,** 1885–1903.

Sausen, R., 2000: Aviation impact as part of global climate change. *Proc. Conf. on Aviation, Aerosols, Contrails and Cirrus Clouds (A^2C^3)*, Seeheim, Germany, European Commission, 275–280.

——, K. Gierens, M. Ponater, and U. Schumann, 1998: A diagnostic study of the global distribution of contrails. Part I: Present day climate. *Theor. Appl. Climatol.*, **61,** 127–141.

Schmitt, A., and B. Brunner, 1997: Emissions from aviation and their development over time. *Pollutants from Air Traffic—Results of Atmospheric Research 1992–1997*, U. Schumann et al., Eds., BMBF-Förderzeichen 01 LL 9207/0, DLR-Mitteilungen 97-04, Deutsches Zentrum für Luft- und Raumfahrt e.V. (DLR), 37–52.

Schröder, F., and Coauthors, 2000: On the transition of contrails into cirrus clouds. *J. Atmos. Sci.*, **57,** 464–480.

Schumann, U., 2000: Influence of propulsion efficiency on contrail formation. *Aerosp. Sci. Technol.*, **4,** 391–401.

——, 2002: Contrail cirrus. *Cirrus*, D. Lynch et al., Eds., Oxford University Press, 231–255.

——, and J. Ström, 2001: Aviation impact on atmospheric composition and climate. *European Research in the Atmosphere 1996–2000: Advances in Our Understanding of the Ozone Layer During THESEO*, European Commission, 257–307.

Stuber, N., M. Ponater, and R. Sausen, 2001a: Is the climate sensitivity to ozone perturbations enhanced by stratospheric water vapour feedback? *Geophys. Res. Lett.*, **28,** 2887–2890.

——, R. Sausen, and M. Ponater, 2001b: Stratosphere adjusted radiative forcing calculations in a comprehensive climate model. *Theor. Appl. Climatol.*, **68,** 125–135.

Zhang, Y., A. Macke, and F. Albers, 1999: Effect of crystal size spectrum and crystal shape on stratiform cirrus radiative forcing. *Atmos. Res.*, **52,** 59–75.